

Received November 18, 2019, accepted December 2, 2019, date of publication December 5, 2019, date of current version December 23, 2019.

Digital Object Identifier 10.1109/ACCESS.2019.2957844

# Hexagonal QAM-Based Four-Dimensional AMO-OFDM for Spectrally Efficient Optical Access Network Transmission

HYOUNG JOON PARK<sup>ID</sup>, SOO-MIN KANG<sup>ID</sup>, INHO HA<sup>ID</sup>,  
AND SANG-KOOK HAN<sup>ID</sup>, (Senior Member, IEEE)

Department of Electrical and Electronic Engineering, Yonsei University, Seoul 03722, South Korea

Corresponding author: Sang-Kook Han (skhan@yonsei.ac.kr)

This work was supported by the National Research Foundation of Korea (NRF) grant funded by the Korea Government, Ministry of Science and ICT (MSIT), under Grant 2019R1A2C3007934.

**ABSTRACT** A novel spectrally efficient optical transmission in a passive optical network (PON) with hexagonal quadrature amplitude modulation (QAM)-based adaptive modulated optical (AMO) orthogonal frequency division multiplexing (OFDM) is proposed and experimentally demonstrated. With the help of hexagonal QAM and 4-dimensional (4D) modulation, adaptive bit loading is effectively processed to enhance the total data rate. In this approach, some subcarriers are aggregated to transmit integer bits. To employ hexagonal QAM-based 4D AMO-OFDM, the signal to noise (SNR) ratio is calculated using the measured error vector magnitude of the training signal. In our experiment, hexagonal QAM-based 4D AMO-OFDM transmission with a total data rate of 21 Gbps is demonstrated over a 20 km standard single mode fiber for two optical network units (ONUs). The experimental results show that the total data rate obtained using the proposed method is increased by 14% compared to the conventional square QAM-based AMO-OFDM.

**INDEX TERMS** Multidimensional symbol mapping, hexagonal QAM, orthogonal frequency-division multiplexing (OFDM), adaptive modulation, passive optical network (PON).

## I. INTRODUCTION

Transmission capacity has always been a significant issue in terms of supporting various data-hungry applications to satisfy user demands in passive optical networks (PONs) [1]. Therefore, several studies have been reported that were aimed at enhancing the overall transmission capacity of PONs [2]–[5]. However, flexibility is also a significant issue in optical access networks. Therefore, orthogonal frequency division multiple access (OFDMA)-based PONs have attracted a lot of attention [6]. Due to the use of orthogonal frequency subcarriers in OFDMA-PONs, the overall bandwidth could be separately assigned to different optical network units (ONUs) in a single time slot [7]. Transmitted subcarriers could be allocated to each ONUs according to the data requirements of the ONUs. Moreover, much higher data capacity could be achieved than that is possible with digital optical transmission based PONs due to high order modulation formats [6], [8]. Due to high spectral efficiency and

flexible bandwidth allocation, OFDMA-PONs could effectively accommodate various applications in a PON system.

In OFDMA-PONs, adaptive bit allocation could be employed to improve the transmission capacity for the optical transmission. By employing adaptive bit allocation, which is also known as adaptive bit loading, different orders of quadrature amplitude modulation (QAM) formats can be adaptively modulated on different subcarriers to increase the transmission capacity [9]–[11]. Using adaptive bit allocation, high order QAMs are modulated onto the subcarriers with high signal to noise ratios (SNRs), and low order QAMs are modulated onto subcarriers with low SNRs. Adaptive bit loading in PONs based on square QAM has been reported until recently. However, since the gap between the required SNR of neighboring modulation orders of square QAM is quite large, adaptive bit loading techniques could be more effective with different QAM formats.

In this letter, we propose, for the first time, a 4-dimensional (4D) adaptively modulated optical (AMO)-OFDM based on hexagonal QAMs in PONs. The QAM symbols are mapped into a hexagonal lattice to enhance

The associate editor coordinating the review of this manuscript and approving it for publication was San-Liang Lee.

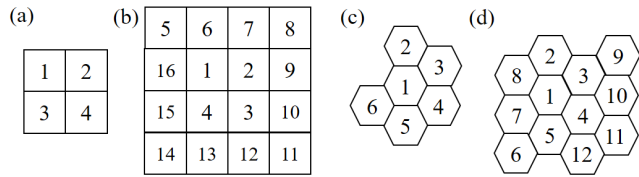


FIGURE 1. Signal constellations of square (a) 4-QAM, (b) 16-QAM, and hexagonal (c) 6-QAM, (d) 12-QAM.

spectral efficiency. Moreover, some subcarriers are merged to transmit 4-dimensional QAMs. 4D hexagonal QAM-based AMO-OFDM was experimentally verified and compared with hexagonal QAM- and square QAM-based AMO-OFDM. We conducted a performance analysis based on the experimental results.

## II. PRINCIPLE OF 4D HEXAGONAL QAM-BASED AMO-OFDM

In conventional square QAMs, symbols are mapped as a rectangular coordinate system as shown in Fig. 1(a) and Fig. 1(b). However, in hexagonal QAMs, symbols are mapped as honeycomb-like structures in two-dimensional signal constellations as shown in Fig. 1(c) and Fig. 1(d). Some studies have been reported that use of hexagonal QAM reduces the peak-to-average power ratio (PAPR), and enhances bit error ratio (BER) [12]–[14]. Due to the high signal constellation density of hexagonal QAM symbols, the symbol error rate (SER) of hexagonal QAM is better than that of conventional square QAMs at the same signal to noise ratio (SNR) as shown in Fig. 4. Therefore, if we transmit symbols using square QAM, larger SNR is required than using hexagonal QAM to satisfy same BER. Thus, transmission throughput could be increased using hexagonal QAM.

However, the orders of conventional QAM are quite discrete. To transmit integer bits on a subcarrier, the number of QAM symbols has to be to the power of 2. Therefore, the number of constellation points is doubled when a bit is added to a subcarrier such as 4-QAM, 8-QAM, 16-QAM. Due to the discrete steps, energy efficiency would be deteriorated. It means that if the measured SNR of optical channel is a bit smaller than required SNR of 64-QAM, only 32-QAM could be transmitted via the optical channel regardless of power loading. Therefore, we added decimal bit QAMs, such as 6-, 12-, 23-, 46-, and 91-QAM that are to the 2.5th, 3.5th, 4.5th, 5.5th, and 6.5th power of 2, respectively. Due to the structure of hexagonal QAMs, decimal bit QAMs could be efficiently mapped into constellations as shown in Fig. 2. However, two decimal bit loaded subcarriers have to be aggregated to transmit integer bits. Fig. 3 shows the algorithms of the proposed technique. In Fig. 3, 5 subcarriers are allocated to ONU1 and 4 subcarriers are allocated to ONU2. The first, fourth, and fifth subcarriers, which are allocated to ONU1, are transmitting integer bit loaded QAMs. Meanwhile, the second and third subcarriers transmit 6 QAM and 23 QAM, respectively. Since the two subcarriers are

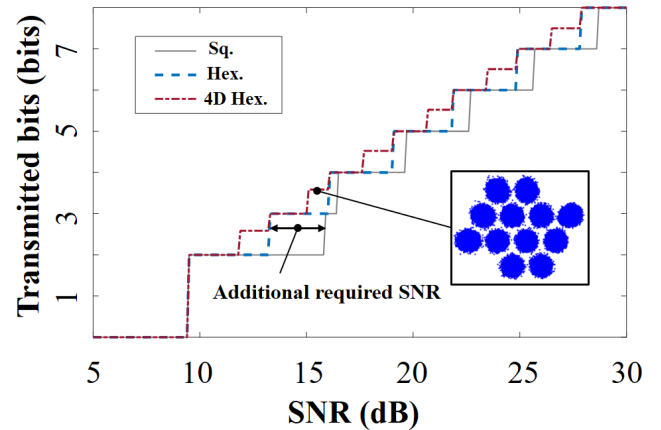


FIGURE 2. Comparison of QAM order between hexagonal QAM and square QAM for SNR variation.

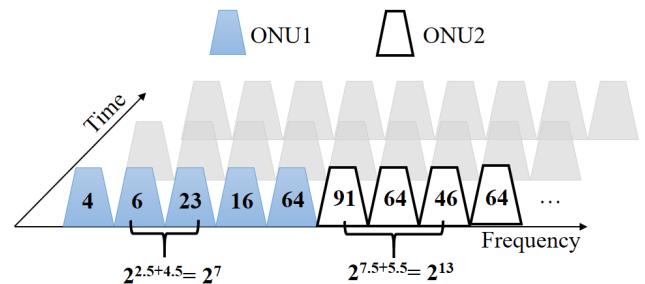


FIGURE 3. Principle of the proposed 4D adaptive bit loading in PON systems with two ONUs.

orthogonal to each other, each two in-phase axes and two quadrature phase axes from second and third subcarriers could become four orthogonal axes by the orthogonality in terms of phase and frequency. Therefore, the aggregated second and third subcarriers could express 138 ( $6 \times 23$ ) numbers of 4D constellation symbols, which could transmit 7 bits. Since the 4D aggregation is employed in partial subcarriers, we refer to this as 4D modulation.

Employing this 4D hexagonal QAM modulation, 3.5 bits or 4.5 bits could be transmitted by a subcarrier. Therefore, the optical transmission system could efficiently modulate different orders of QAMs in each subcarrier. By measuring the SNR to BER graph of each order of QAM, the maximum applicable square QAM, hexagonal QAM, and 4D hexagonal QAM order with respect to the SNR value is confirmed, as shown in Fig. 2. To transmit 4 QAMs, nearly the same SNR is required to satisfy the quality of service (QoS). However, to transmit high order square QAMs, an additional amount of SNR is required than hexagonal QAMs. Also the additional amount of SNR increases as modulation QAM order increases [15], [16]. Moreover, decimal bit loading QAMs enables to transmit additional 0.5 bits at some range of SNR. Therefore, adaptive bit loading could be more efficient using 4D hexagonal QAM compared to square QAM and hexagonal QAM.

## III. EXPERIMENTAL SETUP

Fig. 5 shows the experimental setup of the 4D hexagonal QAM-based AMO-OFDM in a PON system link. Before

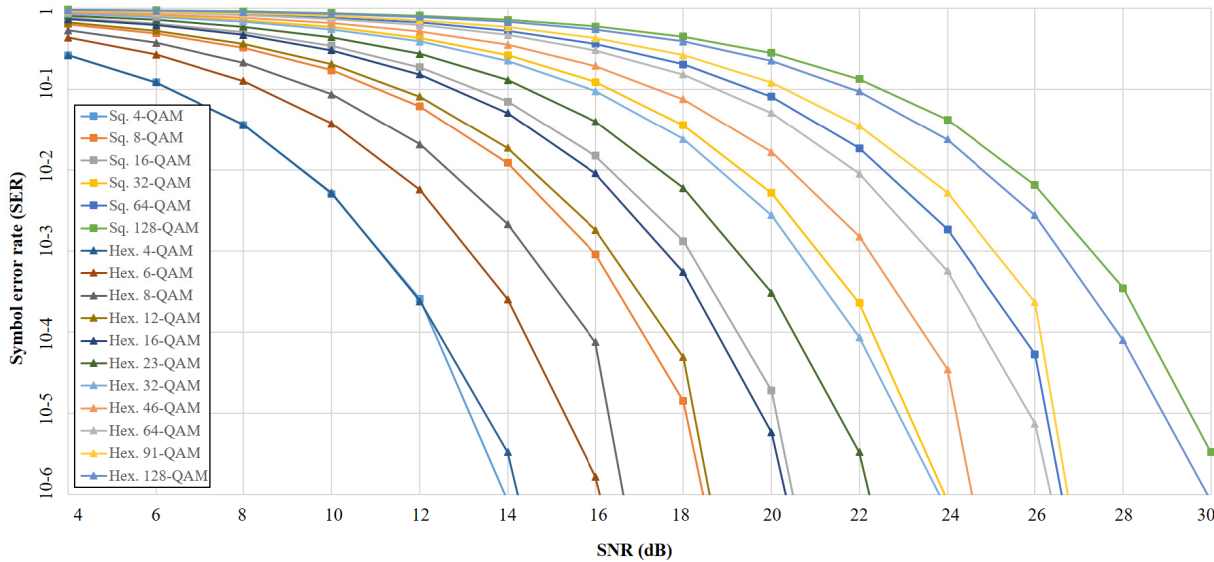


FIGURE 4. Comparison of symbol error rate between square QAMs and hexagonal QAMs (including decimal bit QAMs) according to SNR.

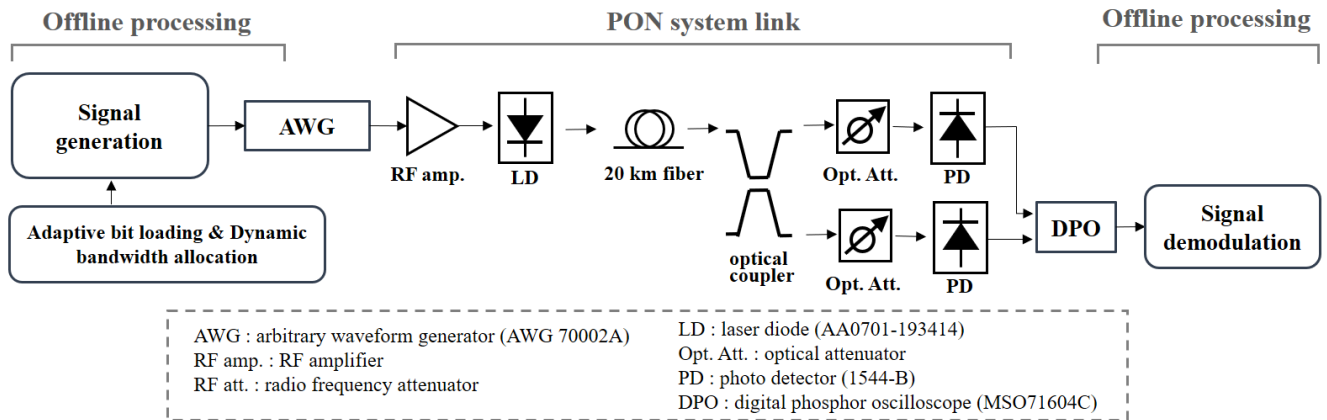


FIGURE 5. Experimental setup of the proposed 4D hexagonal-based AMO-OFDM in a PON system.

transmitting the AMO-OFDM, we measured the SNR gap for hexagonal QAM. Then we measured the SNR at each subcarrier of two ONUs so as to employ adaptive bit loading. The exact values of the SNR for each subcarrier are calculated using the error vector magnitude (EVM) of each transmitted subcarrier. Employing adaptive bit power loading [17], square QAM-based OFDM, hexagonal QAM based OFDM, and 4D hexagonal QAM-based OFDM was generated through offline processing. The subcarrier spacing of the OFDM was 10 MHz. The number of subcarriers was 400 when a 4 GHz bandwidth was modulated. Therefore, IFFT/FFT size was 800 for Hermitian symmetry at 4 GHz bandwidth. Offline processed AMO-OFDM was electrically modulated with 18 G sample per second by an arbitrary waveform generator (AWG). Signal was amplified by radio frequency (RF) amplifier and directly modulated at 1550nm distributed feedback (DFB) laser diode (LD). The 3dB bandwidth of the LD was 10 GHz and output optical power was 0.5 dBm. Also, the temperature of LD was set to room temperature,

which is 25 degrees Celsius. The 4D hexagonal QAM-based AMO-OFDM was optically transmitted through a 20 km standard single mode fiber through intensity modulation in LD. As a proof of concept, a PON system with two ONUs was employed. Therefore, an optical coupler was used to transmit optical signals to the two ONUs. To show the concept of proposed method, we used same PDs for ONU1 and ONU2 to assume that the frequency response of the optical channels between transmitter and two ONUs are the same. After the coupler, an optical attenuator was used to regulate the power of the received optical signal at photo detector (PD). The optical signal received at the PD and was converted into electric signal. The electrical signal was converted into digitized signal using a digital phosphor oscilloscope. Before symbol de-mapping, channel effect was mitigated employing 1-tap equalizer. In our experiment, bandwidth is evenly allocated to ONU1 and ONU2, since the dynamic bandwidth allocation is not the key topic. The performance of the proposed transmission method was analyzed through offline processing.

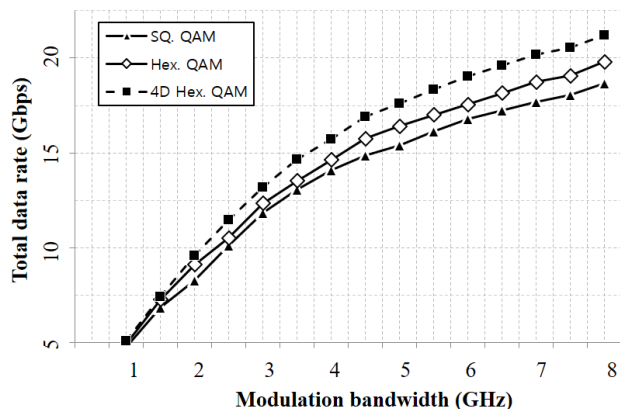


FIGURE 6. Total data rate (ONU1+ONU2) of square QAM-, hexagonal QAM-, and 3D hexagonal QAM-based adaptively modulated OFDM with respect to modulation bandwidth.

#### IV. RESULTS AND DISCUSSION

To confirm the performance enhancement of the 4D hexagonal QAM-based AMO-OFDM in a PON system link, the overall data rate of a conventional square QAM-based OFDM, hexagonal QAM-based OFDM, and hexagonal QAM-based 4D OFDM were compared. By comparing the hexagonal QAM-based AMO-OFDM and square QAM-based AMO-OFDM, the effect of the hexagonal QAM lattice could be confirmed. By comparing the 4D hexagonal QAM-based AMO-OFDM and hexagonal QAM-based AMO-OFDM, the influence of decimal bit loading (also be referred to as 4D modulation) could be confirmed. To verify the comparison in different environments, the transmission performance was compared according to the modulation bandwidth and the received optical power at the PD.

When the received optical power at the PD was fixed at -1.4 dBm, the transmission performance was compared according to the modulation bandwidth. Because the total power of the electrical output at the RF amplifier was constant, the power of a single subcarrier decreased as the modulation bandwidth increased. Fig. 6 shows the transmission performance terms of the overall data rate for ONU1 and ONU2, with different modulation bandwidths employed. When the modulation bandwidth is narrow, the overall data rate is low due to the lack of transmitted subcarriers. When the modulation bandwidth is 1.5 GHz, the hexagonal QAM-based AMO-OFDM scheme achieves 6.4 % higher data rate than the square QAM-based AMO-OFDM. However, the 4D hexagonal QAM-based AMO-OFDM scheme achieves 2 % higher transmission than hexagonal QAM-based AMO-OFDM. Therefore, the high efficiency of the hexagonal lattice is more effective than decimal bit loading at 1.5 GHz bandwidth. This implies that if the SNR of the overall modulated frequency band is nearly flat, indicating that adaptive bit loading is less effective. When the modulated bandwidth is 7.5 GHz, the overall data rate for the 4D hexagonal QAM-based AMO-OFDM scheme is 14 % higher than that of square QAM-based AMO-OFDM. More specifically, the total data rate of the hexagonal QAM-based AMO-OFDM

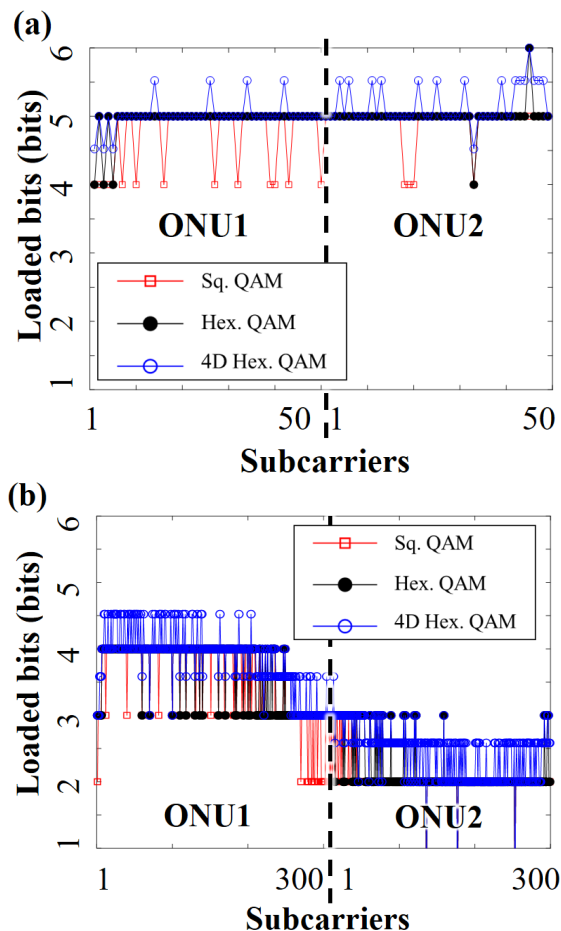
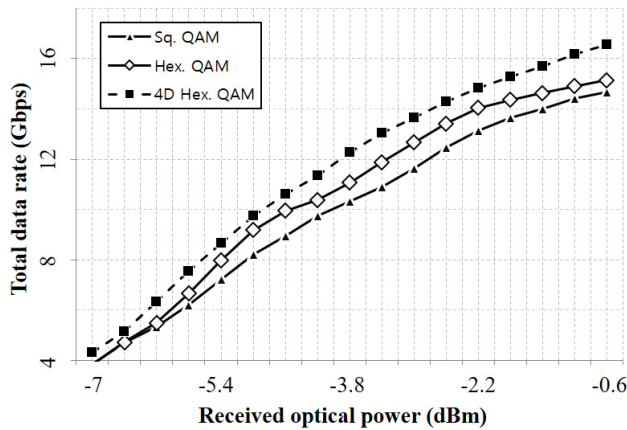


FIGURE 7. Transmitted bits in each subcarrier, at (a) 1 GHz and, (b) 6 GHz modulation bandwidth.

scheme is 5.4 % higher than that of the square QAM-based AMO-OFDM, and the total data rate of the 4D hexagonal QAM-based AMO-OFDM is 7.7 % higher than that of the hexagonal QAM-based AMO-OFDM. This means that decimal bit loading is significant in enhancing data rate when a large bandwidth is employed to transmit signals.

Using 4D hexagonal QAM-based AMO-OFDM improves the total data rate by an average of 12.6 %. Loaded bits for each subcarrier are shown in Fig. 7. In Fig. 7(a), high order QAMs are modulated onto subcarriers at a narrow bandwidth. The Fig. 7(a) shows that 5.5 bits are loaded onto several of the subcarriers employing 4D hexagonal QAM-based AMO-OFDM. On the other hand, hexagonal QAM and square QAM could not transmit 5.5 bits or 6 bits at all the subcarriers. Therefore, 4D hexagonal QAM based AMO-OFDM could transmit more overall bits than other AMO-OFDMs. In Fig. 7(b), the bit loading profile is quite different due to the large modulation bandwidth. More bits are loaded onto subcarriers at low frequencies while fewer bits are loaded at high frequencies. Since the 4D hexagonal QAM-based AMO-OFDM scheme could effectively load bits onto subcarriers, a lot of subcarriers load about half bits more than other AMO-OFDM subcarriers.



**FIGURE 8.** Total data rate of square QAM-, hexagonal QAM-, and 3D hexagonal QAM-based adaptively modulated OFDM with respect to received optical power.

To compare the transmission performance with a fixed modulation bandwidth, the number of subcarriers is fixed at 400, while the modulation bandwidth of the signal is fixed at 4 GHz. Fig. 8 shows the transmission performance terms for the overall data rate for ONU1 and ONU2, with different received optical powers at the PD. Since hexagonal 4 QAM is almost similar to square 4 QAM, the transmission performance at low received optical powers is almost the identical. At any received optical power, the total data rate for the 4D hexagonal QAM-based AMO-OFDM is higher than that of hexagonal QAM or square QAM-based AMO-OFDM. As shown in Fig. 9(a), most of the subcarriers in the square QAM-based AMO-OFDM scheme transmit 4 QAMs. Conversely, majority of the subcarriers in the 4D hexagonal-based AMO-OFDM transmit 6 and 8 QAMs. The total data rate for the 4D hexagonal QAM-based AMO-OFDM is 14.8 Gbps at received optical power of -2.2 dBm. To transmit the same data rate employing the square QAM-based AMO-OFDM, 2 dB of additional received optical power is needed, since 14.6 Gbps is transmitted at -0.6 dBm. Therefore, the optical power dynamic range could be widened more than 1.6 dB by proposed technique. When the received optical power is -5.8 dBm, the enhancement of the data rate is maximized. The total data rate of the square QAM-based AMO-OFDM is 6.2 Gbps while that of the 4D hexagonal QAM-based AMO-OFDM is 7.5 Gbps. Therefore, the overall data rate is increased by approximately 21%. The total data rate was 16.6 Gbps at received optical power of -0.6 dBm and a bandwidth of 4 GHz. As shown in Fig. 9(b), the average bit load is 4.2 bit per subcarrier at -0.6 dBm using 4D hexagonal QAM-based AMO-OFDM. At 0.6 dB, the average loaded bits for hexagonal QAM-based AMO-OFDM and square QAM-based AMO-OFDM are 3.79 and 3.67, respectively. Even though only about a half-bit more load is added at -0.6 dBm, the total data rate is enhanced by an average of 13 %, since high order QAMs are modulated onto the subcarriers. By varying the received optical power at the PD, the total data rate of the 4D hexagonal QAM-based AMO-OFDM is

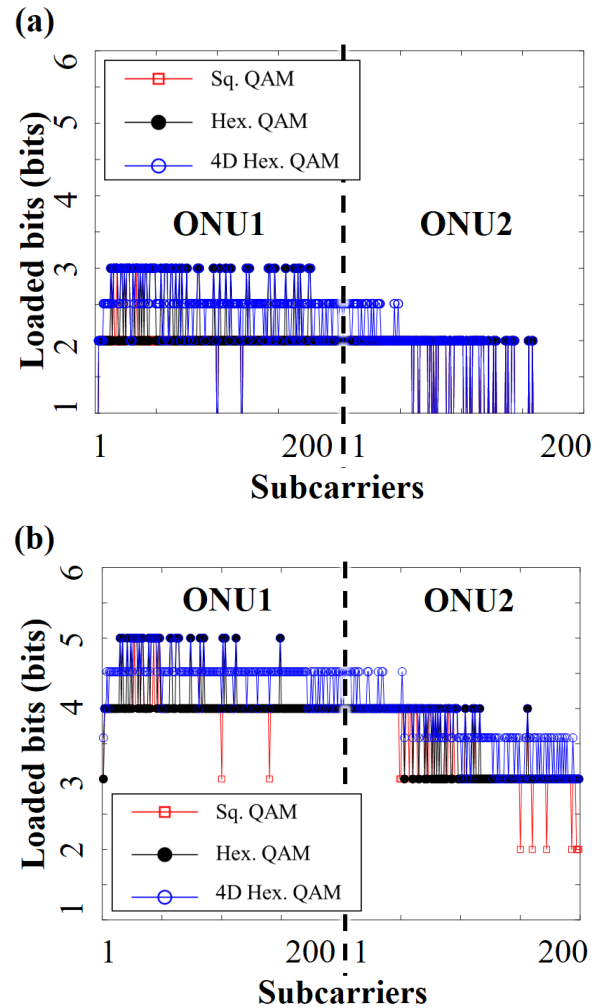


**FIGURE 9.** Transmitted bits in each subcarriers, at (a) -5.8 dBm and, (b) -0.6 dBm of received optical power.

improved on average 9 % compared to hexagonal QAM-based AMO-OFDM, and 16 % compared to square QAM-based AMO-OFDM. Because of the experimental limitations, we just proved that data rate could be improved to 21 Gbps by proposed method. However, the proposed method is scalable in environments with wider bandwidth.

**V. CONCLUSION**

We proposed and experimentally demonstrated a 4D hexagonal QAM-based AMO-OFDM scheme in a PON system. With the help of decimal bit loading QAMs and hexagonal QAMs, adaptive bit loading can effectively be utilized to enhance transmission performance. To transmit decimal bit loaded QAMs, two subcarriers are combined to generate a new orthogonal axis that effectively turns it into a 4D modulation system. However, the combination is processed only at decimal bit loaded subcarriers; thus, the proposed method is named as 4D modulation. The transmission performance of the proposed technique was compared to that of conventional AMO-OFDM and hexagonal QAM-based

AMO-OFDM using a PON system with two ONUs. When the received optical power is -5.4 dBm, the total data rate for the 4D hexagonal QAM-based AMO-OFDM is 8.7 Gbps and the total data rate of the square QAM-based AMO-OFDM is 7.2 Gbps. Therefore, the enhancement in the overall data rate by the proposed method is 20 %. On average, the total data rate for the 4D hexagonal QAM-based AMO-OFDM is 16 % higher than that for the square QAM-based AMO-OFDM. This is a significant increase of data rate in a PON system without employing wavelength or polarization division multiplexing. Therefore, compared to conventional modulation methods, the 4D hexagonal QAM-based AMO-OFDM makes it possible to gain higher spectral efficiency in identical SNR environments. Hence, the proposed technique could be effective for PON systems that require higher data rates and flexibility.

## REFERENCES

- [1] T. Koonen, "Trends in optical access and in-building networks," presented at the ECOC, 2008.
- [2] L. Shi, D. Li, J. He, L. Deng, M. Cheng, M. Tang, S. Fu, M. Zhang, P. P. Shum, and D. Liu, "Experimental demonstration of a 10 Gb/s non-orthogonal multi-dimensional CAP-PON system based on the ISI and CCI cancellation algorithm," *Opt. Lett.*, vol. 41, no. 17, pp. 3988–3991, 2016.
- [3] A. M. Velazquez-Benitez, J. C. Alvarado, G. Lopez-Galmiche, J. E. Antonio-Lopez, J. Hernández-Cordero, J. Sanchez-Mondragon, P. Sillard, C. M. Okonkwo, and R. Amezcua-Correa, "Six mode selective fiber optic spatial multiplexer," *Opt. Lett.*, vol. 40, no. 8, pp. 1663–1666, Apr. 2015.
- [4] D. W. Kwon, S. M. Kang, H. J. Park, and S. K. Han, "Spectral efficiency enhancement in SNR-limited PON system based on SSB 3D modulation," *Microw. Opt. Technol. Lett.*, vol. 59, no. 7, pp. 1765–1772, 2017.
- [5] Z. Li, L. Yi, X. Wang, and W. Hu, "28 Gb/s duobinary signal transmission over 40 km based on 10 GHz DML and PIN for 100 Gb/s PON," *Opt. Express*, vol. 23, no. 16, pp. 20249–20256, 2015.
- [6] N. Cvijetic, D. Qian, J. Hu, and T. Wang, "Orthogonal frequency division multiple access PON (OFDMA-PON) for colorless upstream transmission beyond 10 Gb/s," *IEEE J. Sel. Areas Commun.*, vol. 28, no. 6, pp. 781–790, Jul. 2010.
- [7] B. Skubic, J. Chen, J. Ahmed, B. Chen, L. Wosinska, and B. Mukherjee, "Dynamic bandwidth allocation for long-reach PON: Overcoming performance degradation," *IEEE Commun. Mag.*, vol. 48, no. 11, pp. 100–108, Nov. 2010.
- [8] R. P. Giddings, X. Q. Jin, E. Hugues-Salas, E. Giacomidis, J. L. Wei, and J. M. Tang, "Experimental demonstration of a record high 11.25 Gb/s real-time optical OFDM transceiver supporting 25 km SMF end-to-end transmission in simple IMDD systems," *Opt. Express*, vol. 18, no. 6, pp. 5541–5555, 2010.
- [9] T. N. Duong, N. Genay, M. Ouzzif, J. L. Masson, B. Charbonnier, P. Chanclou, and J. C. Simon, "Adaptive loading algorithm implemented in AMOOFDM for NG-PON system integrating cost-effective and low-bandwidth optical devices," *IEEE Photon. Technol. Lett.*, vol. 21, no. 12, pp. 790–792, Jun. 15, 2009.
- [10] E. Giacomidis, A. Kavatzikidis, A. Tsokanos, J. M. Tang, and I. Tomkos, "Adaptive loading algorithms for IMDD optical OFDM PON systems using directly modulated lasers," *J. Opt. Commun. Netw.*, vol. 4, no. 10, pp. 769–778, 2012.
- [11] L. Nadal, M. S. Moreolo, J. M. Fàbrega, A. Dochhan, H. Griefßer, M. Eiselt, and J. P. Elbers, "DMT modulation with adaptive loading for high bit rate transmission over directly detected optical channels," *J. Lightw. Technol.*, vol. 32, no. 21, pp. 3541–3551, Nov. 1, 2014.
- [12] M. Tanahashi and H. Ochiai, "A multilevel coded modulation approach for hexagonal signal constellation," *IEEE Trans. Wireless Commun.*, vol. 8, no. 10, pp. 4993–4997, Oct. 2009.
- [13] L. Rugini, "Symbol error probability of hexagonal QAM," *IEEE Commun. Lett.*, vol. 20, no. 8, pp. 1523–1526, Aug. 2016.
- [14] A. Malacarne, F. Fresi, J. Klamkin, and L. Poti, "Versatile offset-free 16-QAM single dual-drive IQ modulator driven by binary signals," *Opt. Lett.*, vol. 37, no. 19, pp. 4149–4151, 2012.
- [15] N. Kumar, P. K. Singya, and V. Bhatia, "ASER analysis of hexagonal and rectangular QAM schemes in multiple-relay networks," *IEEE Trans. Veh. Technol.*, vol. 67, no. 2, pp. 1815–1819, Feb. 2018.
- [16] P. K. Singya, N. Kumar, and V. Bhatia, "Impact of imperfect CSI on ASER of hexagonal and rectangular QAM for AF relaying network," *IEEE Commun. Lett.*, vol. 22, no. 2, pp. 428–431, Feb. 2018.
- [17] P. S. Chow, J. M. Cioffi, and J. A. C. Bingham, "A practical discrete multitone transceiver loading algorithm for data transmission over spectrally shaped channels," *IEEE Trans. Commun.*, vol. 43, nos. 2–4, pp. 773–775, Feb./Mar./Apr. 1995.



**HYOUNG JOON PARK** received the B.S. and M.S. degrees in electronic engineering from Yonsei University, Seoul, South Korea, in 2014 and 2016, respectively, where he is currently pursuing the Ph.D. degree in electrical and electronic engineering. His current research interests include multidimensional optical transmission, OFDMA-PON, and next-generation access networks.



**SOO-MIN KANG** received the B.S. degree in electronic engineering from Sogang University, Seoul, South Korea, in 2014, and the M.S. degree in electrical and electronic engineering from Yonsei University, Seoul, in 2016, where she is currently pursuing the Ph.D. degree in electrical and electronic engineering. Her current research interests include coherent optical access networks, passive optical networks, and software-defined optical networks.



**INHO HA** received the B.S. and M.S. degrees in electronic engineering from Yonsei University, Seoul, South Korea, in 2017 and 2019, respectively, where he is currently pursuing the Ph.D. degree in electrical and electronic engineering. His research interests include wireless/wireline convergence and next-generation mobile front haul.



**SANG-KOOK HAN** received the B.S. degree in electronic engineering from Yonsei University, Seoul, South Korea, in 1986, and the M.S. and Ph.D. degrees in electrical engineering from the University of Florida, Gainesville, FL, USA, in 1994. From 1994 to 1996, he was with the System IC Laboratory, Hyundai Electronics, where he was involved in the development of optical devices for telecommunications. He is currently a Professor with the Department of Electrical and Electronic Engineering, Yonsei University. His current research interests include optical devices/systems for communications, optical OFDM transmission systems, passive optical networks, optical networks, and visible-light communication technologies.

• • •